

Influence of Strain Rate on Tensile Characteristics of SUS304 Metastable Austenitic Stainless Steel

Xifeng LI, Jun CHEN[†], Liyan YE, Wei DING and Pengchao SONG

Department of Plasticity Technology, School of Materials Science and Engineering, Shanghai Jiao Tong University, Shanghai 200030, China

[Manuscript received 9 April 2013, in revised form 20 May 2013]

© The Chinese Society for Metals and Springer-Verlag Berlin Heidelberg

The microstructure characteristics and plastic deformation behavior of SUS304 metastable austenitic stainless steel sheets have been investigated during tensile process at different strain rates at room temperature. The yield stress continuously increases with strain rates due to low fraction of martensite transformed from austenite at 0.2% plastic stain. While the ultimate tensile stress (UTS) and elongation gradually decreases and then slightly increases with increase in strain rate from 0.0005 s^{-1} to 0.1 s^{-1} , which is attributed to the variation of the martensite fraction that is affected seriously by adiabatic heating. A higher temperature increase in the tensile specimens restricts the martensitic transformation at high strain rate. The strain rate of 0.1 s^{-1} is considered as a transition deformation rate from quasi-static state to plastic forming, where the transformed martensitic content is very small in a higher strain rate range. Anomalous stress peaks in the later half stage of deformation occur at a very low strain rate (*i.e.*, 0.0005 s^{-1}) result from X-shaped strain localization repeatedly sweeping over the specimen. With increasing strain rates, the variation of dimple number density follows similar trend as that of UTS and ductility because martensite fraction mostly influences void nucleation and growth.

KEY WORDS: SUS304 metastable austenitic stainless steel; Strain rate; Mechanical properties; Martensite fraction; Dimple

1. Introduction

Metastable austenitic stainless steels are widely used as engineering materials due to high corrosion resistivity, beautiful appearance and superior formability. Plastic deformation during forming can lead to a deformation-induced transformation from the original ductile austenite phase to the stronger α' martensite (bcc or bct) and ϵ martensite (hcp)^[1]. Generally, the martensite formation depends on the chemical composition, temperature, grain size, stress state, strain and strain rate^[2–4]. Actually, a few experiments and simulations have been implemented to study the martensitic transformation affected by the strain rate during tensile deformation. Hedström *et al.*^[5] investi-

gated the strain-rate dependence of the strain-induced martensitic transformation and the stress partitioning between austenite and α' martensite in AISI 301 stainless steel during tensile loading. They found that the strain-rate sensitivity of the strain-induced martensitic transformation was high and moderate strain rates of 0.01 s^{-1} would suppress the α' martensite transformation due to adiabatic heating of the tensile specimens. Haušild *et al.*^[6] characterized the kinetics of deformation-induced martensitic transformation in AISI 301 stainless steel and measured magnetic properties, acoustic emission and temperature increase during tensile test at different strain rates. They concluded that yield stress increases and ultimate tensile stress (UTS) decreases with increasing strain rate and elongation has a maximum at $0.005\text{--}3 \text{ s}^{-1}$. The similar experimental results were reported by Shen *et al.*^[7]. They investigated the microstructure characteristics and deformation behavior of 304L stainless steel during tensile deformation at

[†] Corresponding author. Prof., Ph.D.; Tel.: +86 21 62813432; Fax: +86 21 62826575; E-mail address: jun.chen@sjtu.edu.cn (Jun CHEN)

Table 1 Chemical composition (wt.%) of JIS-SUS304 stainless steel sheet investigated

| C | Si | Mn | P | S | Ni | Cr | Al | Fe |
|------|------|------|-------|-------|------|-------|------|------|
| 0.07 | 0.47 | 1.94 | 0.028 | 0.001 | 8.29 | 16.59 | 1.05 | Bal. |

two different strain rates. Instead, Das *et al.*^[8,9] studied the formation and nucleation mechanism of deformation induced martensite during tensile deformation of 304LN stainless steel at various strain rates. They indicated that yield stress steadily increased with increase in strain rate and UTS remained almost constant until strain rate exceeding 0.1 s^{-1} . Additionally, Zhang *et al.*^[10] investigated anomalous plastic deformation and martensitic transformation in type 304 metastable austenitic stainless steel sheets during tensile loading at a very low strain rate. They observed the anomalous stress peaks on the stress-strain curve in the later half stage of plastic deformation. Overall, the influence trend of strain rate on tensile properties of metastable austenitic stainless steels reported in the afore-mentioned literature is inconsistent and controversial. Therefore, it is necessary to further study the tensile characteristics at various strain rates. In this study, the deformation characteristics of SUS304 metastable austenitic steel sheet at different strain rates were investigated by tensile tests. The effect of strain rate on mechanical properties, temperature increase, martensitic transformation and microstructural variation were investigated by different techniques.

2. Experimental

Commercially available JIS-SUS304 metastable austenitic stainless steel sheets with a thickness of 1.2 mm were used in this study. The material is cold rolled sheet in shinning annealed final state. The chemical composition of the steel sheet is listed in Table 1. The as-received steel sheet was manufactured into the specimens with a gauge length of 50 mm and a width of 12.5 mm, which were parallel to the rolling direction of the sheets. Uniaxial tensile tests were performed on a Zwick Roell tensile testing machine with 20 kN maximum load capacity fitted with a 50 mm gauge length extensometer at strain rates of 0.0005, 0.001, 0.005, 0.05 and 0.1 s^{-1} at room temperature. It is considered as a quasi-static tensile deformation when the strain rates were in the range of $0.0005\text{--}0.05 \text{ s}^{-1}$. Whereas the strain rate of 0.1 s^{-1} was thought to be relevant about stamping process. All tests were repeated at least three times in order to ensure the repeatability and reproducibility of experimental results. Temperature variation during the tensile tests was measured by a TES 1310 TYPE-K thermocouple connected with the center of the specimen gauge. The volume fraction of α' martensite phase along the gauge section was measured from the fractured tensile specimens with a Ferritescope FMP30 instrument. According to the magnetic induc-

tion method in the Ferritescope, a low frequency alternating magnetic field generated by the excitation coil interacts with the magnetic phase in the specimen. The change of the magnetic field induces a voltage in the measuring coil proportional to the martensite content. Fractured tensile specimens were longitudinally sectioned adjacent to the fracture surface. Then they are ground with sandpaper and polished with paste. Optical microstructure was revealed by etching in a solution consist of H_2O , HCl and HNO_3 (4:3:3), and observed by optical microscope. Tensile fracture surfaces were carefully examined by the JEOL JSM-7600F scanning electron microscope (SEM) to record fractographic features. A set of fields were observed at an operating voltage of 20 kV throughout. A suitable magnification (2000 times) was used in all cases so that representative fracture features are recorded.

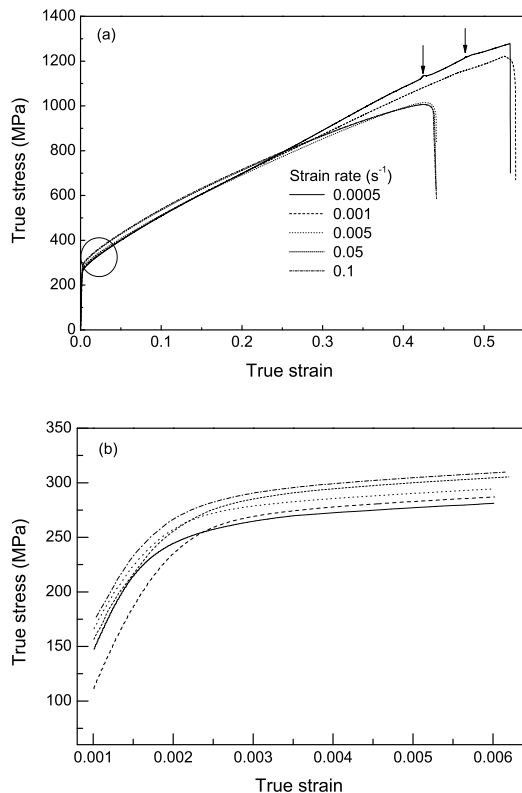
3. Results

Fig. 1 shows the overall room-temperature true stress versus strain curves for the SUS304 stainless steel at five different strain rates. Remarkable hardening can be indicated from the five tensile curves. When strain rate is decreased from 0.1 s^{-1} to 0.005 s^{-1} , the tensile curves few change. Further decreasing from 0.005 s^{-1} to 0.0005 s^{-1} , the yield stress decreases from 284 MPa to 271 MPa, while the ultimate tensile stress increases from 1015 MPa to 1273 MPa. Tensile properties at room temperature obtained with strain rates ranging from 0.0005 s^{-1} to 0.1 s^{-1} are listed in Table 2. These results are in accordance with that found by Haušild *et al.*^[6] and Shen *et al.*^[7] and inconsistent with that reported by Das *et al.*^[8,9]. The effect on elongation is not prominent and almost constant at an average value of 43% until strain rate is less than 0.005 s^{-1} . This trend accords with the results reported by Talonen *et al.*^[11] and Das and Tarafder^[9] while it disaccords with the results reported by Haušild *et al.*^[6]. It is noted that two small anomalous stress peaks occur on the strain-stress curve above 0.43 strain as indicated by arrows. The similar phenomenon was found by Zhang *et al.*^[10]. Whereas UTS and elongation at 0.1 s^{-1} slightly increase compared with that at 0.05 s^{-1} . The strain rate of 0.1 s^{-1} was considered as a deformation rate during sheet metal forming and not ranged in a quasi-static state. This trend is consistent with the results provided by Talonen *et al.*^[11] and Lee and Lin^[12] although this strain rate is much lower than that used by them.

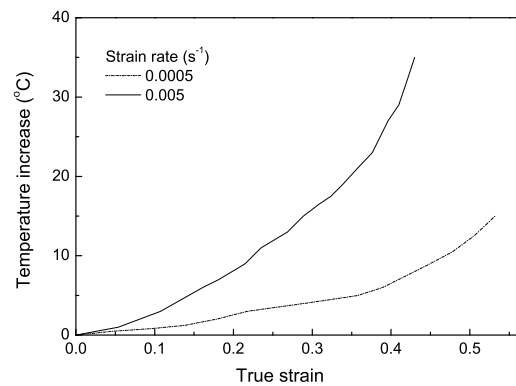
The temperature increase measured at the center of tensile specimens at strain rates of 0.0005 and 0.005 s^{-1} is illustrated in Fig. 2. Obviously, the tem-

Table 2 Tensile properties of SUS304 stainless steel at room temperature at different strain rates

| Strain rate (s^{-1}) | Yield stress (MPa) | Ultimate tensile stress (MPa) | Elongation (%) |
|-----------------------------|-----------------------|----------------------------------|-------------------|
| 0.0005 | 271.2 | 1272.5 | 53 |
| 0.001 | 277.6 | 1207.6 | 52 |
| 0.005 | 283.8 | 1014.5 | 43 |
| 0.05 | 291.9 | 1000.9 | 42 |
| 0.1 | 294.2 | 1010.8 | 43 |

**Fig. 1** True stress-strain curves of SUS304 at various strain rates: (a) tensile curves; (b) magnified image illustrating the yield stress corresponding to circle marked region in Fig. 1(a)

perature increase of tensile specimens at $0.005 s^{-1}$ is higher than that at $0.0005 s^{-1}$. With increase in true strain, the temperature increase steadily improves. A maximum temperature increase is about $35 ^\circ C$ at $0.005 s^{-1}$. The measured data agrees with the calculated and measured results by Haušild *et al.*^[6] and Talonen *et al.*^[11] and simulated results provided by Hedström *et al.*^[5]. Generally, the mechanical energy introduced to the specimen by plastic deformation is almost fully (90%) converted to thermal energy, *i.e.*, adiabatic heating. Furthermore, a remaining portion of the mechanical energy is stored as the elastic energy of the dislocations. Temperature increase also is affected by the transformation heat and heat dissipation by thermal conduction. The transformation heat arises from a free energy change when metastable austenite is transformed to more stable α' martensite phase. In the case of low strain rate (*i.e.*,

**Fig. 2** Measured temperature increase of tensile specimens at strain rates of 0.0005 and $0.005 s^{-1}$

$0.0005 s^{-1}$), the time of thermal conduction lasts long and the heat dissipation approaches the heat generation by adiabatic heating and martensitic transformation. Therefore, the temperature increase is not prominent. On the contrary, the heat generation prevails over the heat dissipation at higher strain rate (*i.e.*, $0.005 s^{-1}$), and the temperature of the tensile specimens obviously increases.

Fig. 3 shows the distribution of α' martensite phase along the gauge sections measured from the fractured tensile specimens at different rates. The results are plotted as a function of distance from the fracture surface. With decrease in the distance from the fracture surface the volume fraction of α' martensite continuously increases at all strain rates. The α' martensite content in the vicinity of the fracture surface is highest. Meanwhile, the increase in the strain rate decreases the α' martensite content in the same distance from the fracture surface. However, the martensite fraction at $0.1 s^{-1}$ is slightly higher than that at $0.05 s^{-1}$, which is listed in Table 2 and correlates with UTS and elongation of the tensile specimens. In addition, the martensite distribution at the strain rate of $0.1 s^{-1}$ is more uniform than that at the quasi-static strain rates. The similar result was found by Talonen *et al.*^[11].

The optical microstructures in as-received state and after tensile deformation at $0.0005 s^{-1}$ and $0.005 s^{-1}$ are shown in Fig. 4. In as-received state, the microstructure is composed of polygonal austenitic grains with typical annealing twins interspersed in some grains. After tensile testing, small martensitic variants grow inside the austenitic grains. Compared

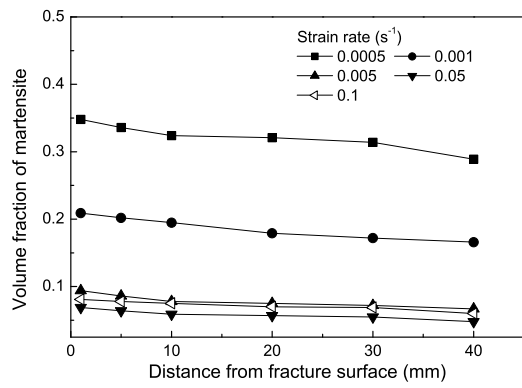


Fig. 3 Volume fraction of α' martensite along the gauge sections of fractured tensile specimens at different strain rates

Fig. 4(b) with Fig. 4(c), the transformed martensite fraction deformed at $0.0005 s^{-1}$ is higher than that at $0.005 s^{-1}$, which well corresponds with the result measured by Ferritescope as plotted in Fig. 3.

To a great extent, the plastic deformation and fracture are influenced by the same set of factors and the fracture surface keeps a clue to the entire deformation process^[13]. Fig. 5 clearly indicates the size of the dimples on the fracture surface changes heavily depending on the strain rates. It is noted that at lower strain rate, dimple number density is higher while dimple size is smaller. A qualitative comparison reveals the dimple number density gradually decreases with increasing strain rate from $0.0005 s^{-1}$ from $0.05 s^{-1}$. Whereas the dimple number density slight increases at $0.1 s^{-1}$

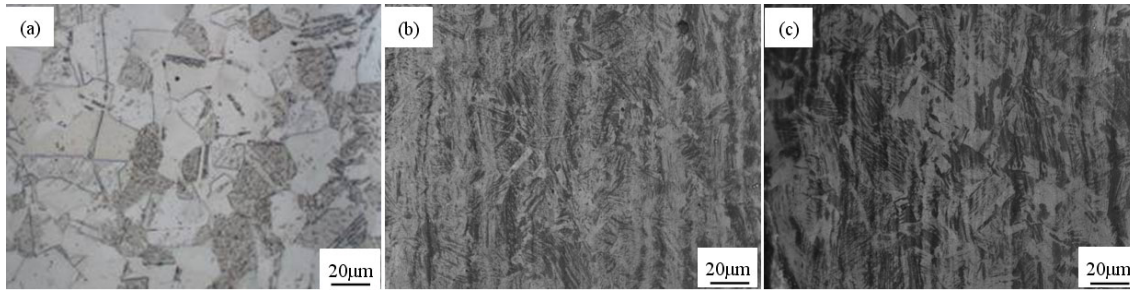


Fig. 4 Optical images show the microstructures of SUS304 stainless steel at different conditions: (a) as-received; (b) after tensile deformed at $0.0005 s^{-1}$; (c) after tensile deformed at $0.005 s^{-1}$

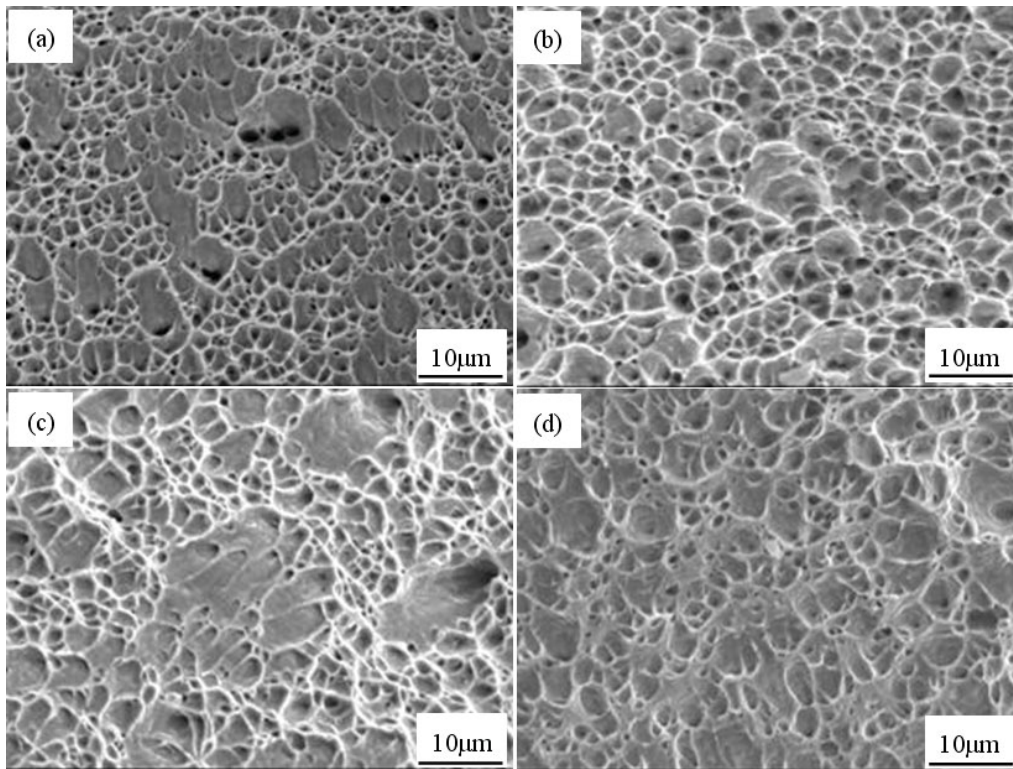


Fig. 5 SEM fractographs of SUS304 tested at different strain rates: (a) $0.0005 s^{-1}$; (b) $0.005 s^{-1}$; (c) $0.05 s^{-1}$; (d) $0.1 s^{-1}$

compared with that at 0.05 s^{-1} . With increasing strain rates, the network of small dimples is steadily replaced by larger dimples, and the density of finer dimples decreases, which corresponds well with the reduced UTS and elongation and the variation of the martensite fraction along gauge sections.

4. Discussion

The change in mechanical properties with strain rates can be rationalized from the viewpoint of dislocation activity and martensitic transformation. It is well known that austenitic stainless steels have high hardening ability due to high dislocation density and the transformation from austenite to martensite. The volume fraction of martensite is varied as a function of true strain. Since the amount of martensitic transformation is small at low strain stage^[2,10,11,14], the dislocation slips control the increase in flow stress during initial tensile deformation. In order to maintain the higher imposed strain rate, the average dislocation velocity needs to be simultaneously increased flow stress. Therefore, yield stress at 0.2% plastic strain gradually increases with increase in strain rates from 0.0005 s^{-1} and 0.1 s^{-1} . At high strain level, the martensitic transformation plays a dominant role in work-hardening mechanism and the martensite predominantly determines the increase in flow stress and ductility due to its high fraction. UTS of some austenitic stainless steels was found to increase linearly with increasing amount of martensite since the induced martensite has a higher strength than the austenite matrix^[15]. Moreover, the transformation induced plasticity (TRIP) effect efficiently delays the onset of necking and significantly increases the uniform and fracture elongation. The maximum amount of formed martensite during tensile deformation is reduced with increase in strain rate from 0.0005 s^{-1} to 0.05 s^{-1} , as shown in Fig. 3 and Fig. 4. Thus UTS and elongation of SUS304 stainless steel decrease with increasing strain rate listed in Table 2.

It is noted that the dislocation movement will be restricted and a local temperature raise will be caused because of dislocation pile-up and tangle when the accumulated plastic strain is increased. The temperature increase in tensile specimens is also caused by exothermic martensitic transformation. Because the generated heat is not transferred out of the specimens rapidly enough, a higher temperature increases at high strain rates. A sample temperature increase of about $35 \text{ }^\circ\text{C}$ at a maximum strain at 0.005 s^{-1} as shown in Fig. 2. Nevertheless, it should be clarified that the measured macroscopic temperature may be lower than the locally true one when an autocatalytic martensitic transformation simultaneously occurs in numerous austenitic grains and large amounts of local heat can be generated^[5,16]. The heating of the tensile specimens can decrease the chemical driving force for the transformation from austenite

to martensite and increase the stacking fault energy (SFE) of austenitic stainless steels. When the SFE is high, the overlapping process of stacking faults becomes irregular and the nucleation of the α' martensite become difficult^[17]. Consequently, the martensite fraction decreases with increasing strain rate from 0.0005 s^{-1} to 0.05 s^{-1} . However, the martensite fraction at 0.1 s^{-1} is slightly higher than that at 0.05 s^{-1} . Correspondingly, similar tendency occurs in UTS since UTS is mainly governed by the martensite fraction in the later stage of tensile deformation. Higher martensite fraction at 0.1 s^{-1} may be attributed to different transformation mechanisms at various strain rate ranges. Talonen *et al.*^[11] have categorized deformation state into three classes according to the magnitude of strain rate. The strain rate of 0.1 s^{-1} may be considered as a transition deformation rate from quasi-static state to plastic forming in the present study. The fraction of martensitic formation is low at plastic forming and dynamic impact rate level. In these ranges, the martensitic formation slowly increases with increasing strain rate. At higher strain rate, multiply-oriented and larger regions of α' martensite have been observed in the shear bands^[12].

Two anomalous stress peaks occur on the stress-strain curve of SUS304 specimen in the later half stage of tensile deformation at 0.0005 s^{-1} . Similar anomalous stress peaks at very low strain rates have been observed by Tominaga *et al.*^[18] using dynamic electronic speckle pattern interferometry and Zhang *et al.*^[10] using in-situ hydrogen and argon releases and scanning probe microscopy. They both considered that the X-shaped strain localization indicating the begin of macroscopically inhomogeneous deformation swept over the specimen repeatedly during deformation and propagated between two anomalous stress peaks, which resulted in the severe α' martensitic transformation in the X-shaped region.

The microstructural mechanism of ductile fracture is associated with nucleation, growth and coalescence of microvoids^[9]. In tensile specimens, voids mainly initiate at the martensite/austenite interfaces along the axis of applied stress where the maximum tensile stress exists. A larger amount of martensite is already formed at low strain rate than at high strain rate as shown in Fig. 3 and Fig. 4. Thus more void nucleation sites are available in the former than in the latter. It is observed that dimple size is smaller in the specimen tested at 0.0005 s^{-1} compared with the specimens tested at 0.05 s^{-1} . With increasing strain rate, the network of fine dimples is gradually replaced by larger dimples. High density of microvoids adjacent to the fracture surface generally involves high plastic strain in this localized necking region. Correspondingly, dimple number density increase towards the fracture surface^[19]. Fig. 5 clearly shows that the dimple number density is higher at 0.0005 s^{-1} than at 0.05 s^{-1} . Additionally, due to slightly higher martensite fraction at 0.1 s^{-1} compared at 0.05 s^{-1} , dimple

size slightly decreases and dimple number density increases, which well correlates with above-mentioned analysis.

A qualitative comparison reveals the variation of UTS and elongation follow similar trend as that of dimple number density. The decrease in dimple density with increase in strain rates results in simultaneous variation in UTS and ductility. Martensite formed by transformation mostly influences void nucleation and growth, and hence UTS and elongation^[20]. At high strain rate, the suppression of martensite by adiabatic heating reduces TRIP effect and the availability of void nucleation sites. Consequently, UTS and elongation decrease while dimple size increases.

5. Conclusions

The conclusions from the present investigation can be summarized as follows:

Yield stress of SUS304 stainless steel increases with increasing strain rate from 0.0005 s^{-1} to 0.1 s^{-1} . This is attributed to dislocation slips and very low martensite fraction at 0.2% plastic strain. Whereas UTS and elongation gradually decrease and then slightly increases, which well correspond with the variation of the total volume martensite fraction determining UTS and elongation. A higher temperature rise hinders martensitic transformation at high strain rate. A maximum increase temperature is about $35\text{ }^{\circ}\text{C}$ at 0.005 s^{-1} , which may be lower than the locally true temperature.

With the increase in strain rate, the dimple number density gradually decreases and then slightly increases, and dimple size follows an inverse trend. This tendency is similar as UTS and elongation since the martensite fraction mostly influences void nucleation and growth.

The strain rate of 0.1 s^{-1} is considered as a transition deformation rate from quasi-static state to plastic forming. Small increase in martensite fraction at higher rates in this strain rate range lead to slight increase in UTS, elongation and dimple number density at 0.1 s^{-1} compared at 0.05 s^{-1} . Anomalous stress peaks in the later half stage of deformation occur at 0.0005 s^{-1} resulted from X-shaped strain localization

repeatedly sweeping over the specimen.

Acknowledgements

The work was supported by the National Natural Science Foundation of China (No. 51105248) and Specialized Research Fund for the Doctoral Program of Higher Education (No. 20090073120058).

REFERENCES

- [1] A. Kundu and P.C. Chakraborti, *J. Mater. Sci.* **45** (2010) 5482.
- [2] S.S. Hecker, M.G. Stout, K.P. Staudhammer and J.L. Smith, *Metall. Trans. A* **13** (1982) 619.
- [3] T.S. Byun, N. Hashimoto and K. Farrell, *Acta Mater.* **52** (2004) 3889.
- [4] A. Etienne, B. Radiguet, C. Genevois, J.M. Le Breton, R. Valiev and P. Pareige, *Mater. Sci. Eng. A* **527** (2010) 5805.
- [5] P. Hedström, L.E. Lindgren, J. Almer, U. Lienert, J. Bernier, M. Terner and M. Odén, *Metall. Mater. Trans. A* **40** (2009) 1039.
- [6] P. Hausild, V. Davydov, J. Drahokoupil, M. Landa and P. Pilvin, *Mater. Des.* **31** (2010) 1821.
- [7] Y.F. Shen, X.X. Li, X. Sun, Y.D. Wang and L. Zuo, *Mater. Sci. Eng. A* **552** (2012) 514.
- [8] A. Das, S. Sivaprasad, M. Ghosh, P.C. Chakraborti and S. Tarafder, *Mater. Sci. Eng. A* **486** (2008) 283.
- [9] A. Das and S. Tarafder, *Int. J. Plast.* **25** (2009) 2222.
- [10] L. Zhang, B. An, T. Iijima, S. Fukuyama and K. Yokogawa, *J. Appl. Phys.* **110** (2011) 033540.
- [11] J. Talonen, P. Nenonen, G. Pape and H. Hänninen, *Metall. Mater. Trans. A* **36** (2005) 421.
- [12] W.D. Lee and C. F. Lin, *Scr. Mater.* **43** (2000) 777.
- [13] A. Das, *Scr. Mater.* **68** (2013) 514.
- [14] S. Ganesh Sundara Raman and K.A. Padmanabhan, *J. Mater. Sci. Lett.* **13** (1994) 389.
- [15] F.B. Pickering, *Int. Met. Rev.* **21** (1976) 227.
- [16] P. Hedström, U. Lienert, J. Almer and M. Odén, *Scr. Mater.* **56** (2007) 213.
- [17] J. Talonen and H. Hänninen, *Acta Mater.* **55** (2007) 6108.
- [18] M. Tominaga, S. Toyooka and H. Kadono, *J. Jpn. Inst. Met.* **71** (2007) 620.
- [19] P. Poruks, I. Yakubtsov and J.D. Boyd, *Scr. Mater.* **54** (2006) 41.
- [20] M. Erdogan and S. Tekeli, *Mater. Des.* **23** (2002) 597.